# Arbitrary single-qubit rotations on chip with twisted waveguides

Fyodor Morozko[1,2],* Andrey Novitsky[2], Alexander Mikhalychev[3], and Alina Karabchevsky[1]†
[1]*School of Electrical and Computer Engineering, Ben-Gurion University of the Negev, Beer-Sheva, Israel*
[2]*Belarusian State University, Minsk, Belarus*
[3]*B. I. Stepanov Institute of Physics, NAS of Belarus, Minsk, Belarus.*

Integrated photonics is a remarkable platform for the realization of quantum computations due to its flexibility and scalability. Here we propose a novel paradigm exploiting twisted waveguides as a building block for polarization-encoded quantum photonic computations on a chip. We unveil a transformation (gate) matrix in the closed form and demonstrate that twisted waveguides can implement arbitrary Bloch sphere rotations. The outcomes of this research may open a new direction in the development of quantum computing architectures on a chip.



*Introduction* The seminal work by Knill, Laflamme, and Milburn (KLM) [1] where the authors proposed a scalable quantum computation protocol using purely linear optics has boosted the exploration of photonics as a platform for implementing quantum information processing. Since the first demonstration of the quantum controlled-NOT (CNOT) gate using the KLM protocol on silicon-on-silica chip in 2008 by Politi *et al* [2] integrated photonics is considered the most promising platform for implementing scalable quantum information processing due to its flexibility in light manipulation in a highly controllable manner [3, 4] and has already reached the level of maturity to allow creating large-scale reconfigurable quantum circuits involving a dozen of qubits [5].

To encode information in a single photon one must use its physical degrees of freedom such as path, momentum, angular momentum, and polarization. For reaching a higher information processing capability per chip footprint it is desirable to make use of the maximum possible number of them. Photon polarization is an always-available natural degree of freedom and is thus among the most widely used encoding mechanisms. To benefit from using an integrated platform it is crucial to perform most or ideally all light manipulations on a chip as most losses occur at a stage of coupling light into a chip or from a chip. However, despite the recognized strength of integrated photonics in controlling light, manipulation of polarization on a chip yet remains elusive. Although integrated photonic polarization-encoded CNOT gate has been demonstrated in laser-written chips, the polarization manipulation in the reported works [6–8] was performed using either bulk or fiber optics. On-chip polarization manipulation schemes based on tilted basis waveguides are typically used serving as waveplates [9, 10] where the waveguide symmetry axis is the optical axis. Such schemes, however, suffer from a number of drawbacks: they are extremely sensitive to fabrication intolerances and due to the cross-section mismatch with normal waveguides exhibit significant coupling losses [11].

A polarization manipulation scheme using carefully designed tapered AlGaAs waveguides performing $\pm 45^\circ$ to circular polarization converter – a quarter waveplate – was proposed by Maltese *et al* [12]. However, this approach is not general and lacks a closed-form description forcing one to perform numerical simulations for any particular design.

It was already recognized in 1979 by Ulrich and Simon that nontrivial polarization dynamics occur in twisted birefringent fibers [13] due to the interplay of linear and circular birefringence, where the former is caused, e.g., by core ellipticity or stress, while the latter is the topological effect owing to twisting as was discussed also in the later works [14, 15]. Due to the recent advances in integrated photonics fabrication technology, especially, in the above-mentioned laser writing, the integrated photonic counterparts of twisted fibers – twisted waveguides – have become reality and has already been suggested as adiabatic polarization rotators [16–18]. The key advantage of twisted waveguides compared to alternative schemes is broadband operation and relaxed constraints on fabrication [17]. As we aim to demonstrate in this letter, twisted waveguides due to their structural elliptical birefringence are capable not only of rotation of linear polarization but rather of general polarization transformation. This allows us to suggest them as arbitrary unitary gates in polarization-encoded quantum information processing circuits. An important strength of twisted waveguides as quantum gates is that polarization transformations are governed by an intuitive analytical model. Furthermore, the laser writing technology within which integrated twisted waveguides are realized in practice is widely used as a platform for quantum information processing due to low losses and unique design flexibility [6–8, 10, 18–21].

*Analytical model of a twisted waveguide* Let us consider a twisted waveguide with a rectangular cross-section and a helix pitch $\Lambda$ as depicted in Fig. 1. It is instructive to use the helical reference frame associated with the twisted waveguide since in this frame the waveguide becomes uniform along the longitudinal coordinate and it becomes possible to split variables in wave equation and, in turn, define an eigenmode. Thus defined eigenmodes of the twisted waveguide then can be approximately represented as a linear combination of the modes of its straight counterpart in the laboratory frame [22, 23]. This approximation is valid if either the pitch $\Lambda$ is much greater than the beat length for the modes of successive orders or the waveguide is a single-mode one. The modes of the twisted waveguide $\left|\tau_\mu\right\rangle$, $\mu = 0, 1$ can be written in the he-

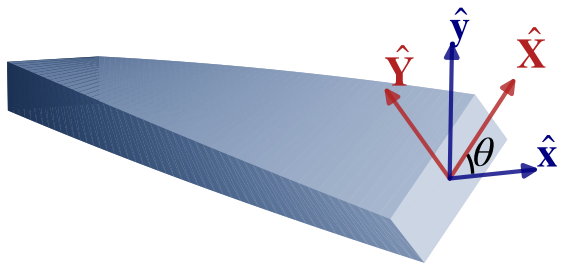


FIG. 1. Transverse basis vectors of the helical ($\hat{\mathbf{X}}, \hat{\mathbf{Y}}$) and laboratory ($\hat{\mathbf{x}}, \hat{\mathbf{y}}$) reference frame.

lical reference frame and, on the other hand, be decomposed in horizontally and vertically polarized modes $|H\rangle$ and $|V\rangle$ of the untwisted waveguide (propagation constants $\beta_h$ and $\beta_v$) as $|\tau_\mu\rangle = M_{\mu 0}|H\rangle + M_{\mu 1}|V\rangle$ or

$$\begin{pmatrix} |\tau_0\rangle \\ |\tau_1\rangle \end{pmatrix} = M \begin{pmatrix} |H\rangle \\ |V\rangle \end{pmatrix}. \tag{1}$$

See details in Supplemental Material [24]. Here $M = \exp(-i\sigma_x\psi/2)$ and $\psi = \arctan(2\alpha/\delta\beta_0)$, where $\sigma_x$ is the Pauli matrix, $\alpha = \theta/L = 2\pi/\Lambda$ is the twist rate, and $\theta$ and $L$ are the twist angle and length of the twisted waveguide, respectively. Parameter $\delta\beta_0 = \beta_h - \beta_v$ accounts for the linear birefringence in the untwisted waveguide, the reciprocal quantity to which being the linear beat length $L_B = 2\pi/\delta\beta_0$. The expression of the matrix $M$ in terms of the Pauli matrix reveals its geometric meaning visualized in Fig. 2(a): the interplay of the linear birefringence induced by unequal cross-section dimensions and topological circular birefringence induced by twisting [13, 14] rotates the eigenmodes around the $x$ axis passing through points $|A\rangle$ and $|D\rangle$ in Fig. 2(a) corresponding to $\pm 45^\circ$ states. In the linear birefringence regime, $\psi \to 0$ corresponds to the "slow" twist $L_B/\Lambda \to 0$ and the modes coincide with horizontally and vertically polarized modes of the untwisted waveguide $|H\rangle$ and $|V\rangle$. In the circular birefringence regime, $\psi = \pi/2$ can be associated with the "rapid" twist behavior, $L_B/\Lambda \to \infty$, in which the modes are circularly polarized, $|R\rangle$ and $|L\rangle$ in Fig. 2(a). Waveguides with square or circular cross-sections possess pure circular birefringence, since the linear one stemming from unequal geometrical dimensions vanishes. In any intermediate case, the mode polarization is elliptical being the mixture of linear and circular polarization. Modes propagation constants of the twisted waveguide can be presented as $\beta_{0,1} = \bar{\beta} \pm \delta\beta/2$, where the average propagation constant is $\bar{\beta} = (\beta_0 + \beta_1)/2 = (\beta_h + \beta_v)/2$ and the elliptical birefringence is defined in terms of the linear birefringence $\beta_0$ and twist rate $\alpha$ as follows

$$\delta\beta = \sqrt{\delta\beta_0^2 + (2\alpha)^2}. \tag{2}$$

The above equation can be depicted geometrically as in the inset of Fig. 2(b). Propagation constants of the modes $|\tau_\mu\rangle$. $\mu = 0, 1$ are shown in Fig. 2(b). Curiously, here we have reproduced the result reported in [25] for twisted photonic crystal fibers: Eigenvalues diverge due to the topological Zeeman effect. The crucial difference from that work is that in our case the eigenvalues do not degenerate in the absence of twisting due to the presence of the linear birefringence.

Transmission of the eigenmodes of the twisted waveguide is associated with the phase advance being given by $|\tau_\mu\rangle \mapsto e^{-i\beta_\mu L}|\tau_\mu\rangle$ or in the matrix form

$$\begin{pmatrix} |\tau_0\rangle \\ |\tau_1\rangle \end{pmatrix} \mapsto D \begin{pmatrix} |\tau_0\rangle \\ |\tau_1\rangle \end{pmatrix}. \tag{3}$$

The phase factors are on the diagonal of the matrix $D = \exp(-i\sigma_z\phi/2)$, where $\sigma_z$ is the Pauli matrix, $\phi = \delta\beta L$ is the accumulated phase difference between the modes (retardance). It should be noted that we have neglected the global phase factor $e^{-i\bar{\beta}L}$ as it does not affect the polarization state. Both the initial and final polarization can be presented also in the basis of horizontal and vertical modes, $|H\rangle$ and $|V\rangle$. In order to transfer to the basis of $|H\rangle$ and $|V\rangle$ we introduce the transformation (1) to Eq. (3) and obtain

$$\begin{pmatrix} |H\rangle \\ |V\rangle \end{pmatrix} \mapsto D_{HV} \begin{pmatrix} |H\rangle \\ |V\rangle \end{pmatrix}, \tag{4}$$

where $D_{HV} = M^\dagger D M$ and $M^\dagger$ is the Hermitian conjugate matrix. As we show in Supplemental Material, the matrix $D_{HV}(\psi, \phi) = \exp(-i(\sigma_z \cos\psi + \sigma_y \sin\psi)\phi/2)$ results in a rotation around the straight line $|\tau_0\rangle \leftrightarrow |\tau_1\rangle$ shown in Fig. 2(a). We remind now that the basis modes $|H\rangle$, $|V\rangle$ are polarized along the transverse basis vectors $\hat{\mathbf{X}}$, $\hat{\mathbf{Y}}$ of the helical reference frame shown in Fig. 1. To obtain the gate matrix, we need to transform the components at the output facet of the waveguide to the laboratory frame. As we demonstrate in Supplemental Material, the transverse components in the two frames are related by means of the rotation matrix in the waveguide transverse plane. This rotation corresponds to the rotation of the Bloch sphere around the $y$ axis (line $|L\rangle \leftrightarrow |R\rangle$ in Fig. 2(a)). Then the transmission matrix in the laboratory frame is the composition of two rotations

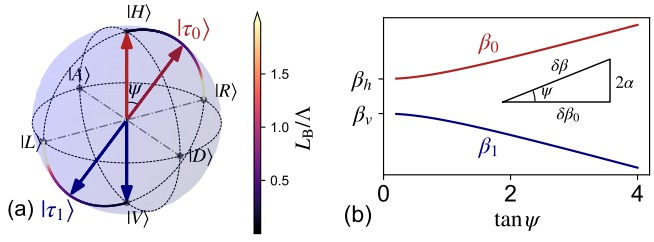


FIG. 2. Eigenvectors (a) and eigenvalues (b) of the eigenmodes of a twisted waveguide as a function of $\psi$. Inset in (b) geometrically represents Eq. (2)

$T(\theta,\psi,\phi) = \exp(-i\sigma_y\theta)D_{HV}(\psi,\phi)$. The two rotations mentioned above are a single rotation on the Bloch sphere by angle $\chi$ around axis $\hat{\mathbf{n}}$ as

$$T = \exp(-i\hat{\mathbf{n}}\cdot\vec{\sigma}\chi/2). \tag{5}$$

The angle $\chi$ is defined by the set of previously introduced angles $\theta$, $\psi$, and $\phi$:

$$\begin{aligned}
\cos\frac{\chi}{2} &= \cos\theta\cos\frac{\phi}{2} + \sin\theta\sin\frac{\phi}{2}\sin\psi,\\
n_x\sin\frac{\chi}{2} &= \cos\psi\sin\theta\sin\frac{\phi}{2},\\
n_y\sin\frac{\chi}{2} &= \cos\frac{\phi}{2}\sin\theta + \cos\theta\sin\frac{\phi}{2}\sin\psi,\\
n_z\sin\frac{\chi}{2} &= \cos\theta\cos\psi\sin\frac{\phi}{2}.
\end{aligned} \tag{6}$$

We provide a derivation of the rotation parameters in Supplemental Material.

In the case of the slow twisting ($\psi \to 0$), the gate $T$, as follows from Eq.(6), reduces to the rotation around the $y$ axis by the angle $2\theta$: $T \to \exp(-i\sigma_y\theta)$. This corresponds to the adiabatic polarization rotation regime. Interestingly, in the work [17] where twisted waveguides were examined as polarization rotators, the authors observed slight ripples in polarization conversion dependency on the twist length having larger amplitude at smaller twist lengths. Those ripples can be explained by deviation from the perfectly adiabatic regime and the presence of noticeable circular birefringence ($\psi \neq 0$). In the case of dominant circular birefringence ($\psi \to \pi/2$) we can see using some algebra of trigonometric functions that the gate reduces to the unity: $T \to 1$. The latter observation expresses the known fact from fiber optics that linear birefringence is necessary to get nontrivial polarization dynamics. This also implies that the waveguide's cross-section should be non-square for the realization of nontrivial polarization conversion performance. The absence of polarization conversion in a rapidly twisted or a square twisted waveguide has an important practical implication: One can always attach a short twisted section at the end facet of the waveguide to compensate for cross-section mismatch due to the rotation of the end facet without affecting the gate performance.

The general, Bloch sphere rotation is described by three independent parameters – Euler angles. The three parameters of the twisted waveguide $\theta$, $\phi$, $\psi$ are however not independent, since Eq.(2) implies a constraint $\phi\sin\psi = 2\theta$. It nevertheless turns out that it is possible to implement an arbitrary rotation with a twisted waveguide approximately but with arbitrary precision, as we demonstrate below.

*Approximating arbitrary unitary operation with twisted waveguides* To estimate how efficiently twisted waveguides can realize different unitary operations (gates) we posed an inverse design problem: For a given ideal unitary operator, namely a Bloch sphere rotation with given Euler angles find the best-twisted waveguide approximation where the twisted waveguide is defined by two parameters: the length $L$ in terms of linear beat lengths $L_B$ and the twist angle $\theta$. As a measure of proximity of two operators, we used gate fidelity proposed in Ref. [26], $F = \frac{1}{2} + \frac{1}{12}\sum_{j=x,y,z}\mathrm{Tr}\left(T\sigma_j T^\dagger U\sigma_j U^\dagger\right)$, where $U$ is the ideal gate and $T$ is its twisted waveguide approximation as defined by (5) and (6). We have performed a scan over all combinations of Euler angles by sweeping azimuthal and rotation angles from 0 to $2\pi$ and sweeping the polar angle from 0 to $\pi$ with some small finite steps effectively covering with a discrete grid all possible single qubit gates and finding the twisted waveguide approximation for each one. The grid dimensions were $33\times65\times17$ for polar, azimuthal and rotation angle giving the total number of gates of 36465. In order for the solutions to be of practical significance we imposed constraints on the twisted waveguide length and twist angle and calculated the worst fidelity $F_{\min}$ over a set of ideal operators as a function of the constraints. We provide the details of the numerical solution to the inverse design problem in Supplemental Material. Fig. 3 summarizes the results of the analysis. Fig. 3(a) shows the worst fidelity $F_{\min}$ among all the designs while Figs. 3(b-d) show worst fidelities for the approximations of rotations around different axes for $\theta_{\max} = 20\pi$ and three values of $L$. The position of a point coincides with the rotation axis while the colors correspond to the worst fidelity over a set of rotation angles [$\chi$ in Eq.(5)] with respect to this axis. Figs. 3(e-g) below show the corresponding fidelity distributions. For all considered constraints, fidelities appear to group near unity whereas increasing the maximum length $L$ reduces the width of the distribution. The results demonstrate that the absolute majority of gates can be indeed approximated with a practical fidelity when twisted waveguides are constrained to have lengths less than a few linear beat lengths and the twist angle of $20\pi$ which corresponds to 10 total twists. State-of-the-art laser-written waveguides typically exhibit birefringences (in terms of modal indices) $\delta n \sim 10^{-5}-10^{-4}$ depending on the particular fabrication process and cross-section dimensions. Such a birefringence ensures the linear beat length $L_B \sim 8-0.8$ cm at wavelength 800 nm [18]. We thus can conclude that laser-written twisted waveguides implementing any possible single qubit gate must be in a millimeter to centimeter size scale comparable to that of the integrated photonic CNOT gates reported earlier [7].

*Two qubit and multi-qubit gates* Although in this Letter we consider only single-qubit operations, the suggested approach can be straightforwardly generalized to the implementation of multi-qubit gates by utilizing more degrees of freedom of a photon e.g. by using path encoding with multiple coupled twisted waveguides or space division multiplexing with multiple modes of the same waveguide. Here we herald only the concept of the twisted-waveguide-based gates. Consideration of multi-qubit gates deserves separate publication.

*Conclusion* To sum up, we have obtained an analytical expression for the transmission matrix of a twisted waveguide which turns out to be a general Bloch sphere rotation. We have shown that twisted waveguides can approximate arbitrary unitary operations with arbitrary precision and reasonable design constraints. This finding allows suggesting twisted waveguide

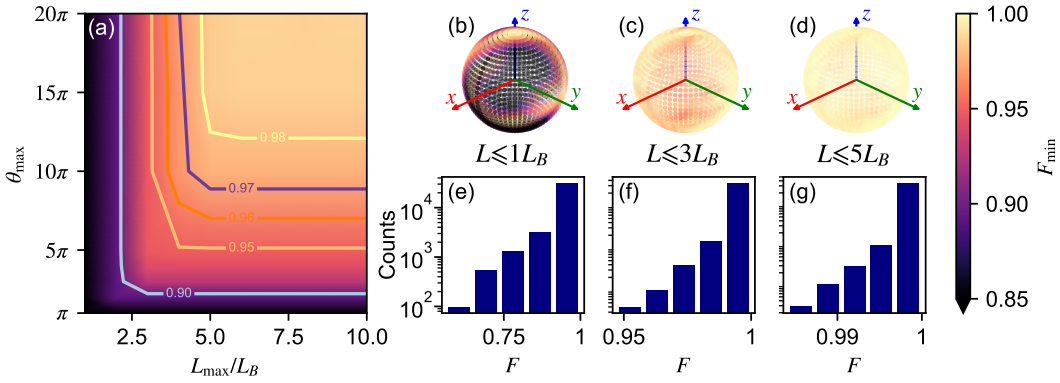


FIG. 3. Twisted waveguide approximation of arbitrary single-qubit gates. (a) shows worst fidelity $F_{\min}$ overall single qubit gates as a function of twisted waveguide design constraints, where $\theta_{\max}$ is the maximum twist angle, $L_{\max}$ is the maximum twist length measured in terms of linear beat lengths $L_B$. (b-d) show the worst fidelity over rotations around a given axis with $\theta_{\max} = 20\pi$ and three different $L_{\max}$ constraints, histograms (e-g) below the spheres visualize the distribution of approximation fidelities.

as a robust yet simple building block for integrated photonic polarization-encoded quantum information processing.

* fedarm@post.bgu.ac.il
† alinak@bgu.ac.il

[1] E. Knill, R. Laflamme, and G. J. Milburn, A scheme for efficient quantum computation with linear optics, Nature **409**, 46 (2001).
[2] A. Politi, M. J. Cryan, J. G. Rarity, S. Yu, and J. L. O'Brien, Silica-on-Silicon Waveguide Quantum Circuits, Science **320**, 646 (2008).
[3] S. Slussarenko and G. J. Pryde, Photonic quantum information processing: A concise review, Applied Physics Reviews **6**, 041303 (2019).
[4] J. Wang, F. Sciarrino, A. Laing, and M. G. Thompson, Integrated photonic quantum technologies, Nature Photonics **14**, 273 (2020).
[5] J. Carolan, C. Harrold, C. Sparrow, E. Martín-López, N. J. Russell, J. W. Silverstone, P. J. Shadbolt, N. Matsuda, M. Oguma, M. Itoh, G. D. Marshall, M. G. Thompson, J. C. F. Matthews, T. Hashimoto, J. L. O'Brien, and A. Laing, Universal linear optics, Science **349**, 711 (2015).
[6] L. Sansoni, F. Sciarrino, G. Vallone, P. Mataloni, A. Crespi, R. Ramponi, and R. Osellame, Polarization Entangled State Measurement on a Chip, Physical Review Letters **105**, 200503 (2010).
[7] A. Crespi, R. Ramponi, R. Osellame, L. Sansoni, I. Bongioanni, F. Sciarrino, G. Vallone, and P. Mataloni, Integrated photonic quantum gates for polarization qubits, Nature Communications **2**, 566 (2011).
[8] J. Zeuner, A. N. Sharma, M. Tillmann, R. Heilmann, M. Gräfe, A. Moqanaki, A. Szameit, and P. Walther, Integrated-optics heralded controlled-NOT gate for polarization-encoded qubits, npj Quantum Information **4**, 13 (2018).
[9] G. Corrielli, A. Crespi, R. Geremia, R. Ramponi, L. Sansoni, A. Santinelli, P. Mataloni, F. Sciarrino, and R. Osellame, Rotated waveplates in integrated waveguide optics, Nature Communications **5**, 4249 (2014).
[10] R. Heilmann, M. Gräfe, S. Nolte, and A. Szameit, Arbitrary photonic wave plate operations on chip: Realizing Hadamard, Pauli-X and rotation gates for polarisation qubits, Scientific Reports **4**, 4118 (2015).
[11] M. F. Baier, *Polarization Multiplexed Photonic Integrated Circuits for 100 Gbit/s and Beyond*, Ph.D. thesis, Technische Universität Berlin (2018).
[12] G. Maltese, Y. Halioua, A. Lemaître, C. Gomez-Carbonell, E. Karimi, P. Banzer, and S. Ducci, Towards an integrated AlGaAs waveguide platform for phase and polarisation shaping, Journal of Optics **20**, 05LT01 (2018).
[13] R. Ulrich and A. Simon, Polarization optics of twisted single-mode fibers, Applied Optics **18**, 2241 (1979).
[14] A. Michie, J. Canning, I. Bassett, J. Haywood, K. Digweed, M. Åslund, B. Ashton, M. Stevenson, J. Digweed, A. Lau, and D. Scandurra, Spun elliptically birefringent photonic crystal fibre, Optics Express **15**, 1811 (2007).
[15] A. Argyros, J. Pla, F. Ladouceur, and L. Poladian, Circular and elliptical birefringence in spun microstructured optical fibres, Optics Express **17**, 15983 (2009).
[16] M. Schumann, T. Bückmann, N. Gruhler, M. Wegener, and W. Pernice, Hybrid 2D–3D optical devices for integrated optics by direct laser writing, Light: Science & Applications **3**, e175 (2014).
[17] Z.-S. Hou, X. Xiong, J.-J. Cao, Q.-D. Chen, Z.-N. Tian, X.-F. Ren, and H.-B. Sun, On-Chip Polarization Rotators, Advanced Optical Materials **7**, 1900129 (2019).
[18] B. Sun, F. Morozko, P. S. Salter, S. Moser, Z. Pong, R. B. Patel, I. A. Walmsley, M. Wang, A. Hazan, N. Barré, A. Jesacher, J. Fells, C. He, A. Katiyi, Z.-N. Tian, A. Karabchevsky, and M. J. Booth, On-chip beam rotators, adiabatic mode converters, and waveplates through low-loss waveguides with variable cross-sections, Light: Science & Applications **11**, 214 (2022).
[19] G. D. Marshall, A. Politi, J. C. F. Matthews, P. Dekker, M. Ams, M. J. Withford, and J. L. O'Brien, Laser written waveguide photonic quantum circuits, Optics Express **17**, 12546 (2009).
[20] T. Meany, M. Gräfe, R. Heilmann, A. Perez-Leija, S. Gross, M. J. Steel, M. J. Withford, and A. Szameit, Laser written circuits for quantum photonics: Laser written quantum circuits, Laser & Photonics Reviews **9**, 363 (2015).
[21] F. Flamini, L. Magrini, A. S. Rab, N. Spagnolo, V. D'Ambrosio, P. Mataloni, F. Sciarrino, T. Zandrini, A. Crespi, R. Ramponi,

and R. Osellame, Thermally reconfigurable quantum photonic circuits at telecom wavelength by femtosecond laser micromachining, Light: Science & Applications **4**, e354 (2015).

[22] A. Nicolet, F. Zolla, and S. Guenneau, Modelling of twisted optical waveguides with edge elements, The European Physical Journal Applied Physics **28**, 153 (2004).

[23] D. M. Shyroki, Exact Equivalent Straight Waveguide Model for Bent and Twisted Waveguides, IEEE Transactions on Microwave Theory and Techniques **56**, 414 (2008).

[24] Supplemental Material.

[25] T. Weiss, G. K. L. Wong, F. Biancalana, S. M. Barnett, X. M. Xi, and P. S. Russell, Topological Zeeman effect and circular birefringence in twisted photonic crystal fibers, Journal of the Optical Society of America B **30**, 2921 (2013).

[26] M. D. Bowdrey, D. K. L. Oi, A. J. Short, K. Banaszek, and J. A. Jones, Fidelity of Single Qubit Maps, Physics Letters A **294**, 258 (2002), arXiv:quant-ph/0201106.

[27] F. Morozko, A. Karabchevsky, and A. Novitsky, Modal theory for twisted waveguides, in *Metamaterials XIII*, edited by K. F. MacDonald, A. V. Zayats, and I. Staude (SPIE, Strasbourg, France, 2022) p. 61.

[28] M. A. Nielsen and I. L. Chuang, *Quantum Computation and Quantum Information*, 10th ed. (Cambridge University Press, Cambridge ; New York, 2010).

[29] R. Storn and K. Price, Differential Evolution – A Simple and Efficient Heuristic for global Optimization over Continuous Spaces, Journal of Global Optimization **11**, 341 (1997).

[30] P. Virtanen, R. Gommers, T. E. Oliphant, M. Haberland, T. Reddy, D. Cournapeau, E. Burovski, P. Peterson, W. Weckesser, J. Bright, S. J. van der Walt, M. Brett, J. Wilson, K. J. Millman, N. Mayorov, A. R. J. Nelson, E. Jones, R. Kern, E. Larson, C. J. Carey, İ. Polat, Y. Feng, E. W. Moore, J. VanderPlas, D. Laxalde, J. Perktold, R. Cimrman, I. Henriksen, E. A. Quintero, C. R. Harris, A. M. Archibald, A. H. Ribeiro, F. Pedregosa, P. van Mulbregt, and SciPy 1.0 Contributors, SciPy 1.0: Fundamental Algorithms for Scientific Computing in Python, Nature Methods **17**, 261 (2020).